Polymer Testing 74 (2019) 216–224

Contents lists available at ScienceDirect

Polymer Testing

journal homepage: www.elsevier.com/locate/polytest

Material Behaviour

Fatigue damage evolution in unidirectional glass/epoxy composites under a cyclic load

Oscar Castro[a,*], Paolo Andrea Carraro[b], Lucio Maragoni[b], Marino Quaresimin[b]

[a] Department of Wind Energy, Technical University of Denmark, Denmark
[b] Department of Management and Engineering, University of Padova, Italy

ARTICLE INFO

Keywords:
Fatigue damage
Damage evolution
Glass/epoxy materials
Broken fibers

ABSTRACT

The initiation and progression of fiber damage in on-axis UD glass/epoxy materials under fatigue loading conditions were studied. Uniaxial tension–tension fatigue tests at different load levels were carried out to monitor the fiber damage evolution through the fatigue lifetime. The damage evolution was quantified by initial fiber breaks, the evolution of fiber breaks, fragmentation and clustering progression. Through qualitative and quantitative analyses, it is shown how the fiber damage evolution depends on the number of cycles, the applied load level and the number of broken fibers during the first cycle.

1. Introduction

Fatigue life estimation of composite materials has been a demanding research field in the last 40 years, as most structures made partially or totally of these materials, such as wind turbine blades, are subjected to cyclic loadings. These composite structures are mainly made of multidirectional laminates consisting of unidirectional (UD) plies with different orientations. The stiffness degradation of these laminates is principally caused by the onset and propagation of matrix cracks in the off-axis UD plies, together with the initiation and propagation of delamination between the different plies [1]. Nevertheless, their structural load-bearing capacity is determined by the on-axis UD plies, which have a different failure mode and a higher fatigue strength than the off-axis ones. Accordingly, if the objective is to predict the fatigue stiffness degradation and failure of multidirectional laminates, it is necessary to predict [1]:

i) the initiation and propagation of off-axis cracks (the crack density evolution),
ii) the initiation and propagation of delamination induced by off-axis cracks, and
iii) the failure of the fibers of the load-bearing plies.

The authors [2] presented a procedure for predicting the crack density evolution, whereas an approach and preliminary results for the prediction of delamination propagation were shown in Ref. [3]. In the present work, the attention is focused on the fiber-related damage mechanisms under on-axis cyclic loading as a fundamental step toward the prediction of the final fatigue life of a multidirectional laminate.

The progressive fiber failure process under cyclic loads is a rather complex issue, particularly considering that, in multidirectional laminates, this process interacts with the damage in the off-axis plies such as transverse cracks and delamination. Therefore, for the definition of a reliable predictive tool for such a complicated phenomenon, it is first necessary to understand how the different fiber-related damage mechanisms initiate and evolve until reaching the final failure.

The on-axis fatigue behavior of UD laminates under tension–tension loading conditions has been studied over many years [4–8]. The different damage mechanisms involved in this type of material under these loading conditions have been identified qualitatively through experiments. Damage in the on-axis UD laminates initiates from the first applied cycle when multiple fiber breaks occur [6,7]. These breaks can occur in different fibers (isolated) or along individual fibers (i.e., fragmentation) due to the statistical strength distribution of the fibers [7]. When the fiber/matrix interface is relatively weak (e.g., in some glass/epoxy materials), fiber/matrix debond cracks initiate at the fiber crack tip due to the high stress concentration on the fiber in the vicinity of the break [6–9]. The debonds start growing with the number of cycles, redistributing in this way the load on the neighboring fibers. When a weak segment in one of the neighboring fibers is overloaded, it may fail and give rise to new debonds [7–9]. In some cases, the debond cracks kink out in the matrix and grow in mode I towards the neighboring fibers, increasing the possibility that new fiber breaks appear due to the increase of local stresses [10]. This damage mechanism has led to the belief that the final failure comes from a critical fracture

* Corresponding author.
E-mail address: osar@dtu.dk (O. Castro).

https://doi.org/10.1016/j.polymertesting.2018.12.027
Received 30 November 2018; Accepted 26 December 2018
Available online 27 December 2018
0142-9418/

plane formed when a critical number of fibers adjacent to the initial fiber break also fail [6,11]. However, there is not enough experimental evidence so far that proves that this is the actual damage mechanism that leads to the final failure in on-axis UD composites under fatigue loading conditions.

Nevertheless, based on the previous damage description of the UD composites, it is clear that progressive fiber breaking is an important phenomenon in the failure process. This is why this topic has received quite a lot of attention and has been studied by several researchers since the 70s considering the behavior of single and multiple fibers embedded in a matrix. The failure progression of single fibers under static loadings has been analyzed experimentally [12–15] and theoretically [16–18]. An important analytical study was that developed by Hui et al. [18]. They developed equations for the evolution of fiber fragments in single fibers loaded under increasing strain by assuming a Weibull distribution for the fiber strength.

However, as fibers are not used as single fibers in real composites but as multiple fibers embedded in a matrix, different experimental [6,11,19–23] and analytical [19,24–26] studies have been carried out to understand how the fiber breaking initiates and evolves in a group of fibers, until reaching the final failure, by considering the effect of fiber interaction. Smith [25] proposed, for example, a probabilistic model that relates the Weibull probability strength distribution function of single fibers with the probability of failure of a composite material made of multiple parallel fibers subjected to quasi-static tension loading conditions. However, Aroush et al. [11] showed by experimental observations that, with specimens made of 125 single fibers, the model proposed by Smith [25] overestimates the critical number of broken fibers needed to lead the final failure of the material. Moreover, the maximum number of fiber breaks in a cluster of broken fibers observed by Aroush et al. in Ref. [11] agreed well with those observed by Swolfs et al. in Ref. [21], where a total of about 5500 UD fibers in the cross-section of $[90/0]_s$ laminates were analyzed.

All previous studies focused on the fiber-breaking progression of the on-axis UD composites under quasi-static loading conditions; fewer studies have considered the fiber-related damage progression under fatigue loading conditions [5,27–34]. In recent years, for example, Garcea et al. [28–31] have worked on the evaluation of the fiber-related damage evolution in notched $[90/0]_s$ carbon/epoxy laminates by using synchrotron X-ray computed tomography. From this evaluation, it was found that few fibers failed in the bulk composite within the 0° plies at peak loads lower than 50% of the ultimate tensile failure stress (UTS); whereas at peak loads higher than 50% UTS a greater number of fibers failed in the bulk composite, whose tendency to form clusters was greater at peak loads higher than 70% UTS. It was shown, indeed, that most fibers failed along 0° ply splits originated at the notch tips, mainly due to the presence and failure of bridging fibers.

Moreover, Zangenberg et al. [32] established a damage progression scheme for UD non-crimp fabric (NCF) under fatigue tensile loading conditions. The NCF materials consisted of UD fiber bundles reinforced with off-axis backing fiber bundles to provide a higher transverse strength, ease of handling and lower manufacturing costs compared to pure UD fibers. Recently, the damage progression scheme established by Zangenberg et al. [32] was expanded by Jespersen et al. [33] based on observations made through 3D x-ray computed tomography analysis. These observations showed that the fiber breaking phenomena were located mainly in regions where the 0° fibers intersect the backing bundles.

A model based on hierarchical fiber bundle failure was recently developed by Alves and Pimenta [35] to predict the failure of UD carbon/epoxy composites under tension-tension cyclic loadings. The model is based on the fact that carbon fibers are fatigue-insensitive and the damage evolves through the propagation of debonds starting from fiber breaks.

Although these studies provide valuable information for further improvements in the ability to predict fiber-related damage in multidirectional laminates, it is still not clear how this type of damage evolves from the first cycle through the fatigue lifetime and leads, possibly, to the final failure. In addition, it is worth mentioning that the experimental works cited above deal with non-purely UD configurations, also in the presence of a notch [28–31], for which it was shown that the fiber-related damage in the bulk material was negligible. As a consequence, "the mechanism for fatigue fiber failure in the bulk composite, and its effect on residual strength is not understood" [30] at present, as well as its evolution from the first cycle to the final failure.

In this frame, the purpose of this work is to investigate the microscale fiber-related damage initiation and progression throughout the lifetime of on-axis UD glass/epoxy laminates under tension–tension fatigue loading conditions. For that, uniaxial fatigue tests under different load levels were carried out, monitoring with optical microscopy the microscale damage evolution throughout the fatigue life. The damage evolution was evaluated, both qualitatively and quantitatively, in terms of initial fiber breaks, evolution of fiber breaks, fragmentation and clustering progression. As previously mentioned, gaining a clear understanding of these phenomena is fundamental for the development of reliable design tools. Accordingly, this work is meant as the first step toward the definition of a procedure for the prediction of fiber-related damage evolution and failure in UD and multidirectional laminates under cyclic loading.

2. Material and methods

Unidirectional (UD) laminates made of glass UT-E500 fibers by Gurit and epoxy RIM-235 resin by Momentive, with lay-up $[0]_6$, were infused and tested. 17 mm wide, 195 mm long, and 1.8 mm thick specimens with a fiber volume fraction of 0.55 were obtained from panels of 200 × 300 mm fabricated by vacuum resin infusion, cured for three days at room temperature and then post-cured at 60 °C for 12 h, Rectangular-shaped carbon-epoxy tabs with 30 mm length and thickness of 3 mm were bonded on both ends of the specimens using an epoxy adhesive.

The UD glass/epoxy specimens were tested under uniaxial tension–tension fatigue loading conditions using a MTS 858 hydraulic machine. The tests were performed in load control with maximum cyclic tensile stresses $\sigma_{x,max}$ of 200, 300, 320, and 340 MPa with a load ratio $R = \sigma_{min}/\sigma_{max} = 0.05$. The tests were repeated twice for each load level, except for $\sigma_{x,max} = 200$MPa case, for which only one test was carried out. Static tests were carried out before the fatigue tests to measure the ultimate tensile failure stress (UTS) of the material, which was found as 432 MPa. It is important to say that the final failure occurred as a consequence of splits originating from the end tabs. Therefore, the ultimate stress value obtained may not be considered as the material strength.

The damage evolution of the material was monitored in terms of stiffness degradation and fiber breaks. The stiffness of the specimens was determined based on the strains measured with a MTS632.29F-30 extensometer with a 25 mm initial length, the stresses calculated from the applied load and the specimen cross-area. In order to monitor the damage evolution in terms of fiber breaks, the front surface of the specimens (Fig. 1) was carefully polished. The polishing process started with P180 sandpaper and finished with a 0.1 μm SiO_2 suspension. The choice of observing the damage development by means of surface microscopic analyses is due the fact that, only with an optical microscope, can micro-

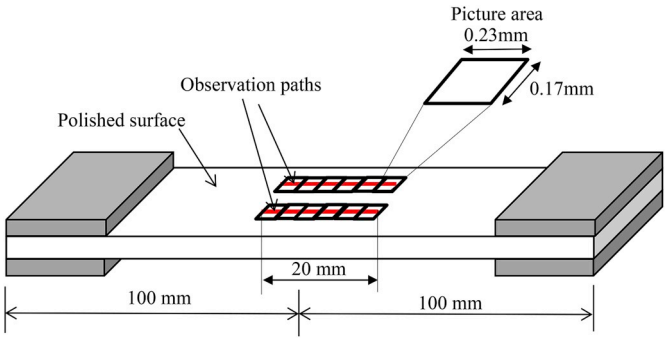

Fig. 1. Schematic of the observation paths.

and sub-microscale details, such as debonds and matrix micro-cracks and shear bands, be revealed (see, for example [36,37]). On the other hand, this limits the observation to a surface and not the volume of the material, thus losing the 3D evolution of damage. This could be overcome by combining optical microscopy with computed tomography (CT) analyses, which were not carried out in the present work.

Before the fatigue tests, the specimens were inspected with an optical microscope to identify possible initial damage, such as matrix micro-cracks and fiber breaks. During each fatigue test, the load was regularly interrupted (i.e., at the 1st, 10th, 100th, 1000th, etc. cycles), and the specimen was removed from the hydraulic machine to be observed with the optical microscope. Around 150 pictures were taken on the polished surface at each interruption, each corresponding to small areas of $0.23 \times 0.17\,\text{mm}^2$. The small areas were located along two 20 mm long observation paths, located far from the tabs, across the mid-length of the specimens (see Fig. 1). From the pictures, around 1000 fibers per specimen were analyzed and the number of initial fiber breaks, the evolution of the density of broken fibers, the presence of clusters and the fragmentation evolution were quantified throughout the fatigue life.

3. Results and discussion

In this section, the results obtained from the fatigue tests are analyzed from qualitative and quantitative points of view. In the qualitative analysis, different damage scenarios observed in terms of fiber breaks, fragmentation, increasing opening, matrix yielding and debonding are

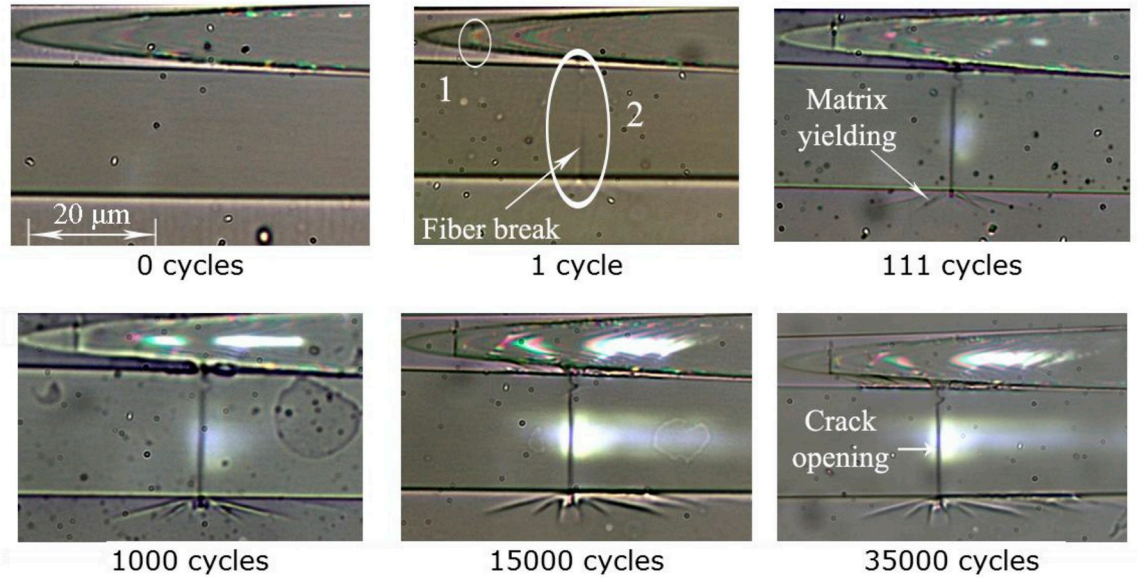

Fig. 2. Damage evolution under $\sigma_{x,max}$ = 300MPa, specimen No 1.

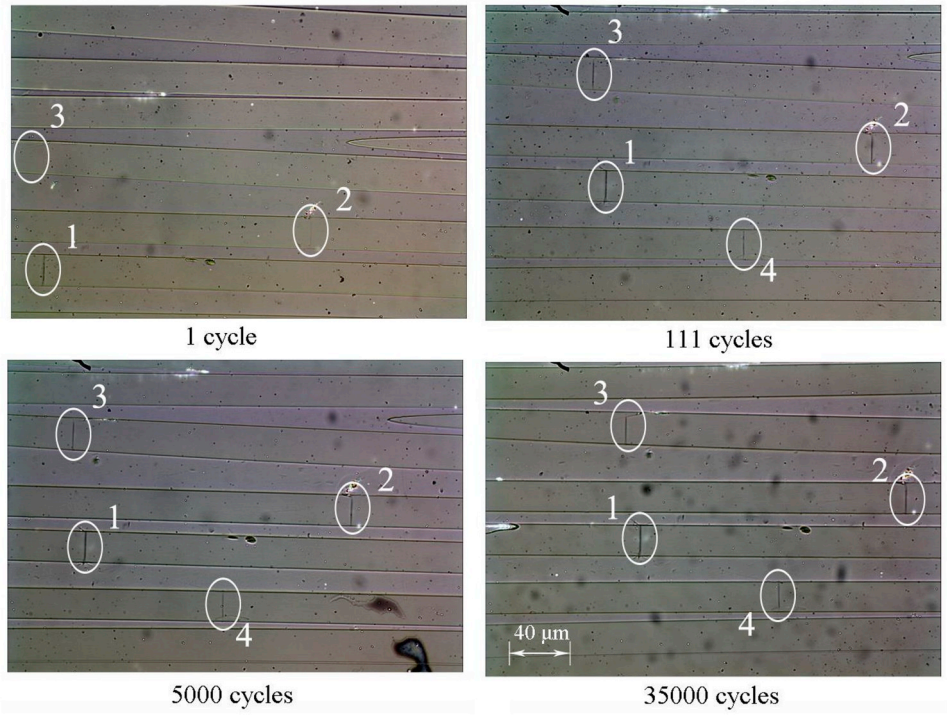

Fig. 3. Damage evolution under $\sigma_{x,max}$ = 300MPa, specimen No 1.

described. In the quantitative analysis, a discussion on the stiffness and the evolution of the fiber breaks during the fatigue life is presented.

3.1. Qualitative description of damage scenarios

The damage scenarios observed from the specimens were in agreement with those described in Refs. [4,7,8]. For all specimens, the fatigue damage initiated during the first cycle when some fibers failed at the weakest locations (see Figs. 2–6), which were sometimes related to the presence of local defects (as will be shown later). This fiber breaking occurred at applied maximum stresses lower than the static stress to failure of the fiber due to the statistical strength distribution.

Close to the fiber breaks, shear yielding or fiber/matrix debonding developed due to high shear stresses in the interface region. These progressive mechanisms resulted in a redistribution of stresses in the area close to the fiber break, causing either arrest or continuation of the

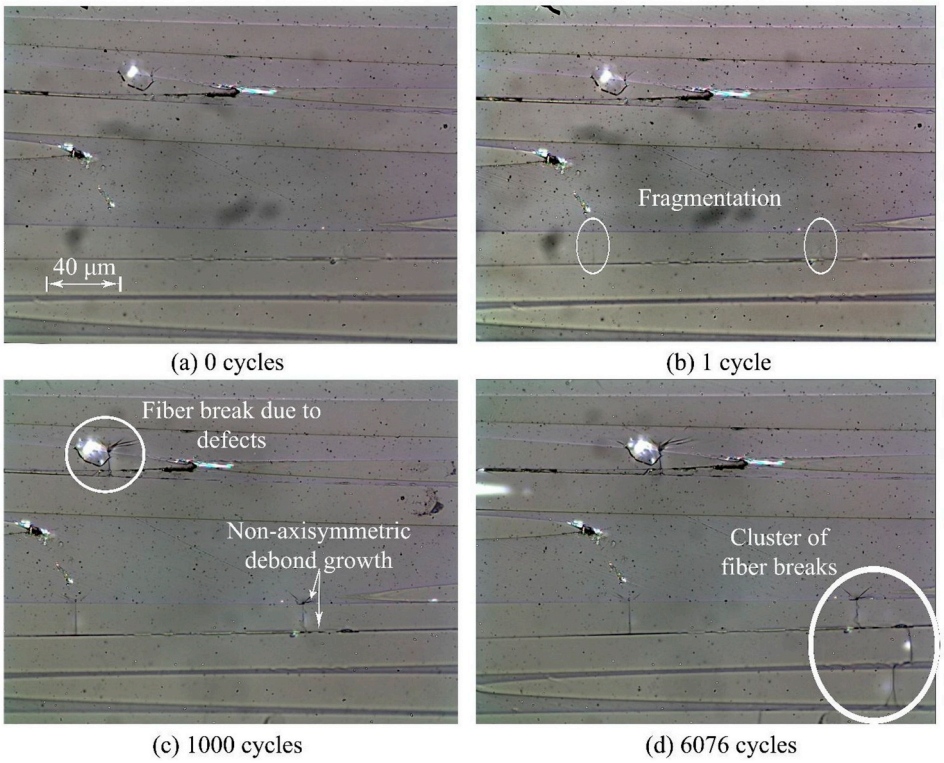

Fig. 4. Damage evolution under $\sigma_{x,max}$ = 320MPa, specimen No 1.

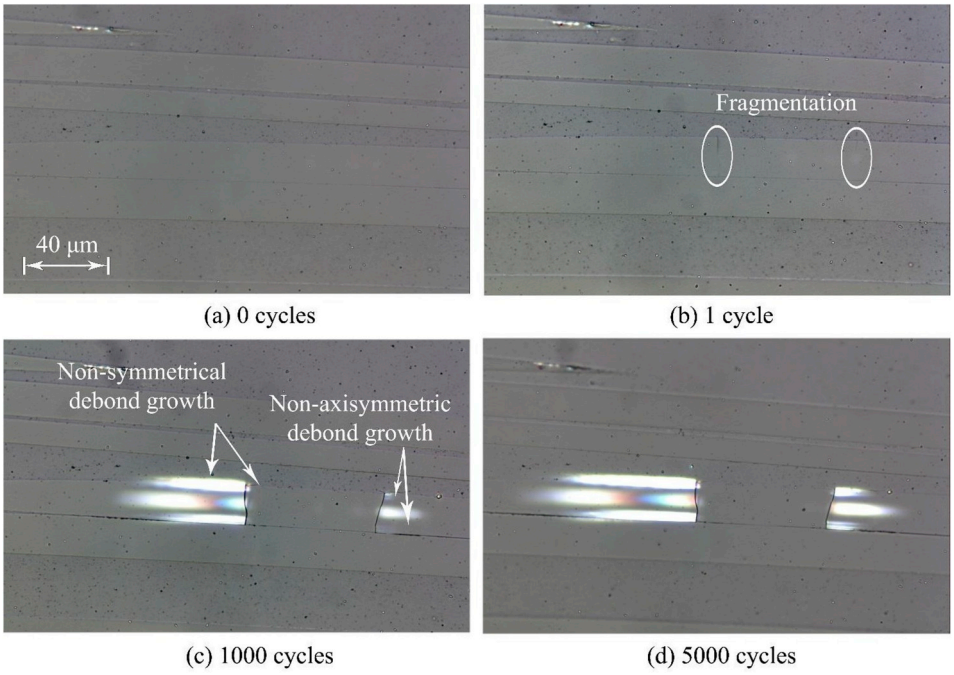

Fig. 5. Damage evolution under $\sigma_{x,max}$ = 320**MPa**, specimen No 2.

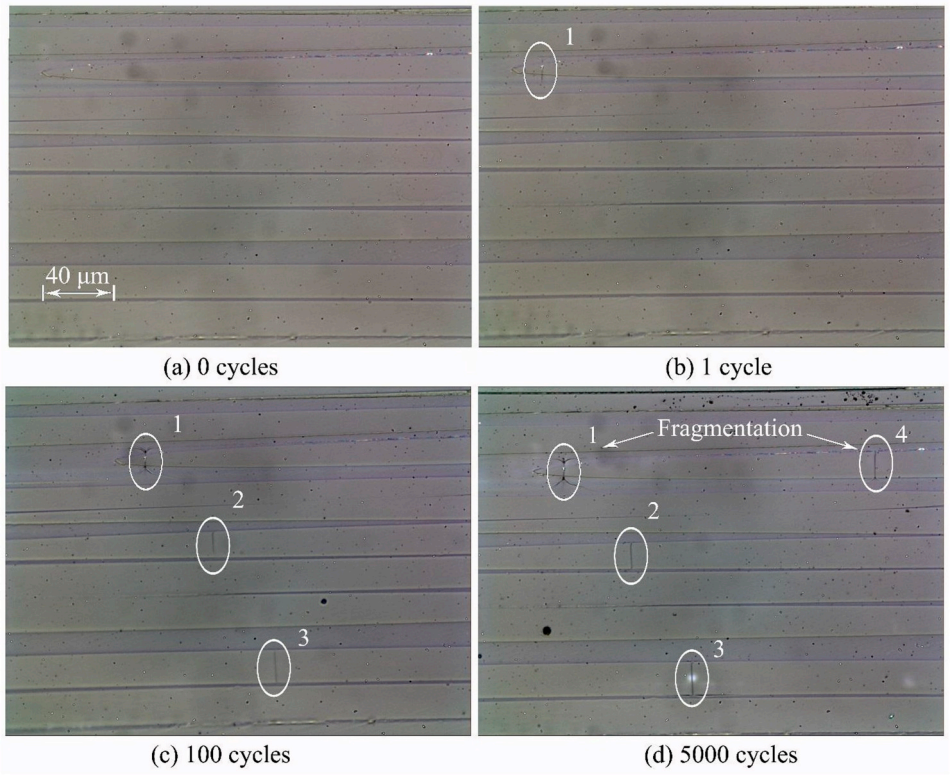

Fig. 6. Damage evolution under $\sigma_{x,max}$ = 320**MPa**, specimen No 2.

damage process depending on the applied load level.

For the lower load levels (i.e., $\sigma_{x,max}$ = 200MPa and 300MPa), matrix yielding was observed at the fiber crack tip (see e.g. in Fig. 2). As shown in Fig. 2, the extension of the yielded zone, characterized by the presence of shear bands in the matrix, propagated along the fatigue life as a result of the energy dissipation, which also contributed to the local stress redistribution and the increase of the residual crack opening. In fact, as shown in Fig. 2, the fiber crack initiated in the first cycle became increasingly visible as the number of cycles increased. However, for lower load levels, no fiber/matrix debonding was observed throughout the fatigue life. This could indicate that the debonds stopped growing at a short distance from the fiber breaks because the threshold needed to continue propagating was not reached. As no debond growth occurred, the stress redistribution caused by the growing shear bands affected only the segments of the neighboring fibers close to the fiber break, decreasing the probability of new fiber breaks. This could be the reason why no, or few, new fiber breaks occurred at the lower load levels (see Figs. 2 and 3).

In contrast, for higher load levels (i.e., $\sigma_{x,max}$= 320 MPa and 340MPa), it was possible to observe fiber/matrix debonds growing from some fiber breaks right after the first cycle, in addition to the matrix yielding at the tip of the fiber break (see Figs. 4–6). As the debonds grew, the redistribution of the stresses affected, not only the segments of the neighboring fibers close to the fiber break, but also those close to the debond tip, causing failure in the weak segments when their local strength was exceeded (see e.g. in Fig. 4-d). In fact, a tendency to form clusters of adjacent fiber breaks was observed in some cases. Such clusters propagated when new breaks in the neighboring fibers appeared, which sometimes joined together by matrix cracks that grew in mode I from the tip of short debonds belonging to the previous broken fibers (see Fig. 4-d). This agrees with what was discussed in Ref. [10], where it was found that short debond cracks tend to kink out into the matrix and grow toward the neighboring fibers, thus enhancing the local stress and causing possible breakages in the neighboring fibers.

The initiation and growth of clusters of adjacent fiber breaks has been considered in previous studies [11,21] as one of the main damage mechanisms that lead to the final failure of the material. Aroush et al. in Ref. [11] showed that a critical fracture plane is created in specimens made of 125 single fibers when a critical cluster of broken fiber form, which triggers the catastrophic failure of the composite. However, it is still not clear how many adjacent fiber breaks are needed to create the critical fracture plane. In fact, it is not clear either if this critical fracture plane is the final failure mechanism or if it leads to another more critical mechanism (e.g., instable splitting) that does lead to the final failure. Unfortunately, in this work, it was not possible to identify the final failure mechanism because the test pieces failed with splitting parallel to the fiber direction initiated from the tabs as a result of the high-stress concentrations in these regions. Nevertheless, a quantitative analysis of the formation of clusters along the fatigue life is presented in the next section.

Furthermore, even although the propagation rate of the debond cracks was not quantified in this study, it was observed that the debond propagation rate was not uniform. For example, different debond lengths between the two crack tips of the same broken fiber were observed in some cases as well as a non-axisymmetric debond growing in individual fibers (see Figs. 4 and 5). This is because the debond growth depends on the local interfacial properties, which can vary statistically from one location to another, as well as on the distance between the broken fiber and its neighbor, which is non-uniform [38]. In fact, as discussed in Ref. [39], the shorter the distance between the broken fiber and the neighboring fiber, the higher the Energy Release Rate (ERR) and, as a consequence, the higher the debond growth rate. This can be seen in the fiber fragmented twice in Fig. 4 and the one also fragmented twice in Fig. 5, in which the debonds extended from the two breaks are longer on the side near the neighboring fibers than on the opposite side where there is a higher matrix content.

Moreover, another observed damage mechanism was the fragmentation of single fibers, as shown in Figs. 4–6. In most cases, this phenomenon occurred during the first cycle (see e.g. in Fig. 4-b and 5-b) but in a few others it took place after some applied cycles (see e.g. in Fig. 6-d). However, the fragmentation of single fibers was in general not so common, and the damage was seen to progress mainly by the failure

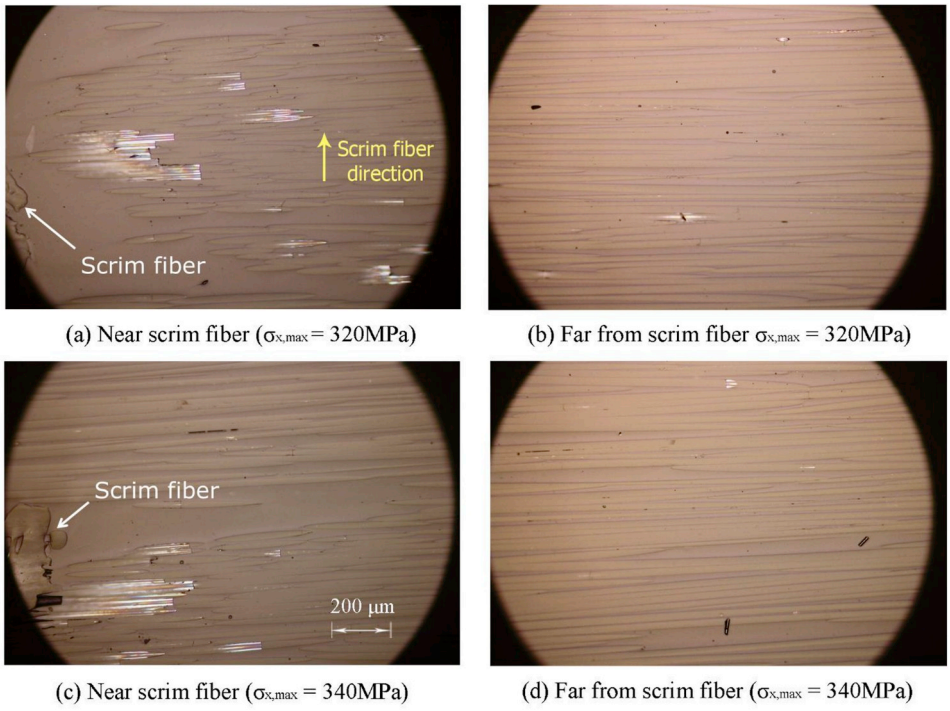

Fig. 7. Comparison between the damage progression in regions close and far to the scrim fiber for different load levels: (a) and (b) $\sigma_{x,max}$ = 320**MPa**; (c) and (d)$\sigma_{x,max}$ = 340**MPa**.

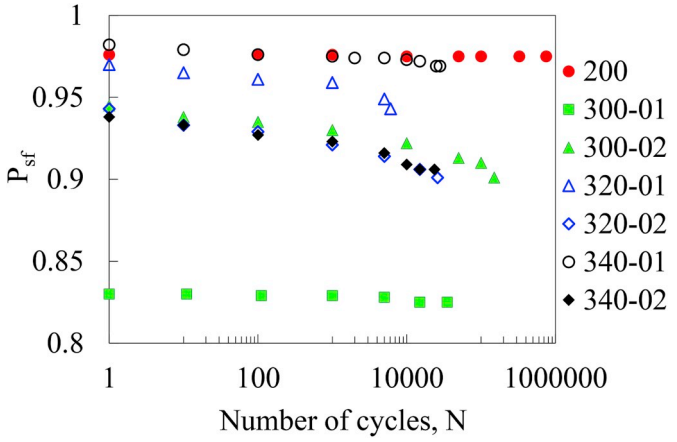

Fig. 8. Evolution of the survival probability along the fatigue lifetime.

of new fibers, as quantified in the next section.

The fragmentation process developed during the first cycle could be compared to that developed under quasi-static loading conditions. In this sense, as in a tensile quasi-static test [12,13,15,24], the tensile stress in the fibers increases when the external load increases during the application of the first cycle, causing some fibers to fail at their weakest points. Consequently, the stresses decay to zero at the fiber breaks but recover their nominal value at some distance from the fiber break [12–15,24,40,41]. Then, as the applied load continue increasing, higher stresses are transferred to the fibers and possible new breakages can develop at other weak points of the already failed fibers [12,13,15,24], see Fig. 4-b and 5-b.

Moreover, in a few cases it was also noticed that some fibers fragmented after some applied cycles, even when debond growth was not observed, which would cause a stress re-distribution along the broken fiber itself (see e.g. in Fig. 6-d). This may be reasonable because of the fact that glass fibers could suffer from fatigue due either to stress corrosion or to fiber-fiber contact (abrasion) [42], which cause slow degradation of the quality of the fiber surface and, therefore, possible failures after some cycles.

In addition to all these observations, it was also found that the propagation of the damage was not uniform along the observation region. In fact, the damage accumulated faster in regions with high concentration of matrix, especially in the regions near the scrim fiber used to hold the primary longitudinal fibers in place during fabrication and handling. This can be seen in Fig. 7, which shows a comparison between the damage progression in regions close to and far to the scrim fiber for different load levels. As shown in Fig. 7, under the same load level, the number of fiber breaks, fragmented fibers, cluster of fiber breaks and debond lengths is always higher in those regions near the scrim fiber. These observations agree well with those presented in Ref. [33] regarding UD non-crimp fabric reinforced polyester composites, in which it was also found that the fiber breaks typically emanate from the matrix-rich regions close to the backing fibers.

As shown in Fig. 7-a and 7-c, in the regions close to the scrim fibers, the debonds tend to grow faster toward the matrix-rich areas where the scrim fibers are located. The increase of the local stresses due to this fast debond growing, along with stress perturbation due to the out-of-plane fiber waviness in these regions, is reasonably the main reason for the greater number of fiber breaks, fragmented fibers and cluster of fiber breaks.

3.2. Quantitative analysis of damage progression

From the qualitative analysis reported in the previous section, it is clear that the number of fiber breaks during the first cycle and its evolution during the fatigue lifetime are significant parameters to be considered in predictive models for UD glass/epoxy composites under fatigue loading. In this section, a quantification of the initial fiber breaks and the progressive appearance of new breakages, both in different fibers (isolated) and along individual fibers (i.e., fragmentation), during the fatigue life is presented. In addition, the effect of the progressive damage on the material stiffness is analyzed.

To quantify the damage state, the specimens were removed from the test machine and observed under the microscope, scanning the polished front surface along two lines with a length of 20 mm (see Fig. 1). Along

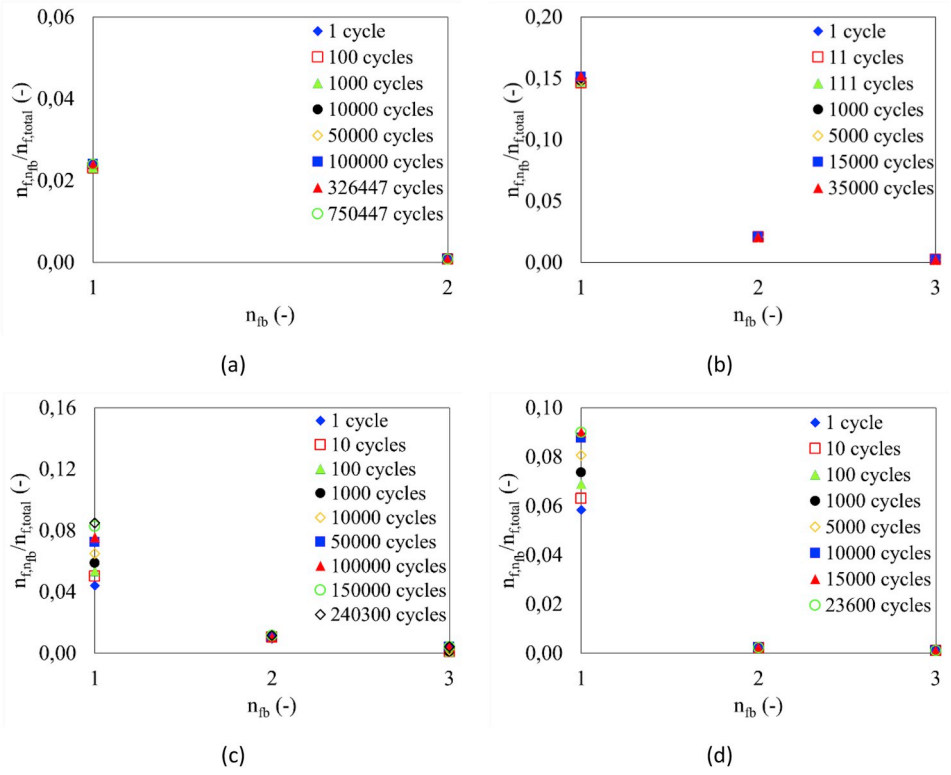

Fig. 9. Normalized number of fiber segments with a given n_{fb} breaks, $n_{f,n_{fb}}/n_{f,total}$, versus n_{fb} through the fatigue life for: (a) $\sigma_{x,max}$ = 200**MPa**; (a) $\sigma_{x,max}$ = 300**MPa**; (c) $\sigma_{x,max}$ = 320**MPa**; (d) $\sigma_{x,max}$ = 340**MPa**.

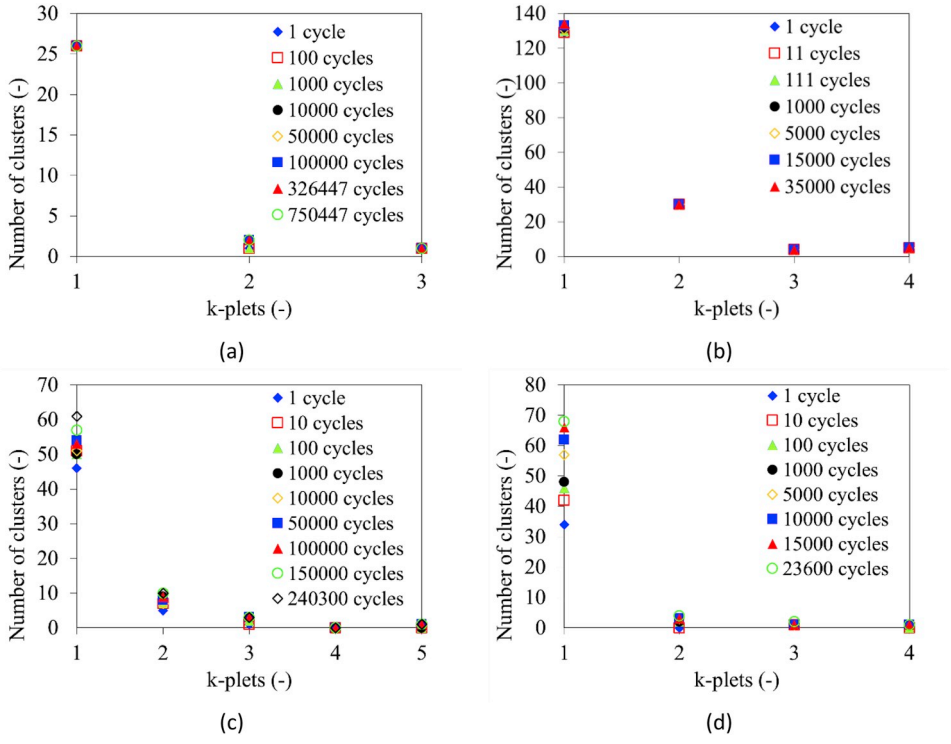

Fig. 10. Number of fiber breaks occurring as singlets (i.e., 1-plet) and clusters (i.e., k **– plets**, $k \geq 2$) for: (a) $\sigma_{x,max}$ = 200**MPa**, (b) $\sigma_{x,max}$ = 300**MPa**, (c) $\sigma_{x,max}$ = 320**MPa**, (d) $\sigma_{x,max}$ = 340**MPa**.

these lines, consecutive pictures were taken and merged to two by two through dedicated software. In this way, the observation paths were divided into sub-regions with a length L_f of about 0.35 mm.

The first important result that can be drawn from this analysis is the probability of survival (P_{sf}) of a fiber segment with length L_f. This was calculated as the sum of the fiber segments without any break, divided by the total number of fiber segments, for each specimen. The resulting probability of survival is plotted in Fig. 8 as a function of the number of

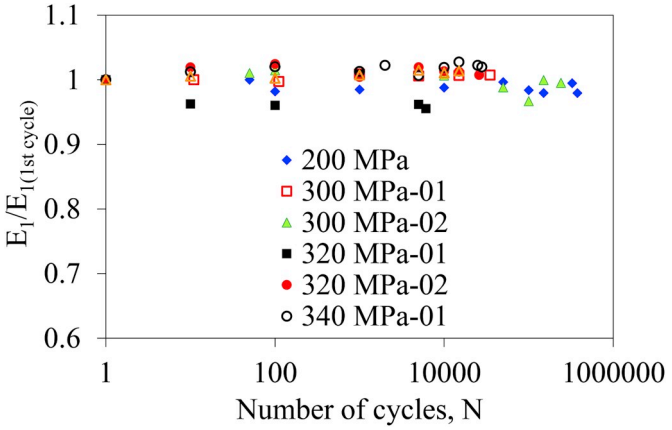

Fig. 11. Normalized stiffness versus number of cycles for different load levels and specimens.

cycles. For the specimen tested at 200 MPa, the curve is flat, meaning that all the breaks occur at the application of the first cycle and no new breaks form in the remaining part of the life. In fact, as mentioned in the previous section, this load level is too low for promoting debond propagation, or to initiate new independent fiber breaks. For the other stress levels, a decreasing trend can be observed, even if most of the damage is again created by the first load cycle. However, for the higher stress levels, damage can be seen to evolve during the fatigue lifetime, and this leads to possible failure after a certain amount of cycles when a critical state is reached.

Furthermore, the broken fibers may show only one break (within the length L_f), or more. In this sense, the fragmentation phenomenon in UD composites can be analyzed in terms of number of breaks (n_{fb}) within a fiber length L_f. The number of fiber segments fragmented by n_{fb} breaks will be identified as $n_{f,nfb}$. Therefore, the probability of finding a fiber segment with n_{fb} breaks can be calculated as $n_{f,nfb}/n_{f,total}$, where $n_{f,total}$ is the total number of fiber segments counted within the observation region. Such a probability is plotted in Fig. 9 as a function of n_{fb} for different applied load levels and number of cycles. It should be noted that the total number of fiber segments, $n_{f,total}$, taken into account for each analyzed case was around 1000, which is believed to be a representative sample size.

As shown in Fig. 9, the higher the number of breaks within the same fiber segment, n_{fb}, the lower the $n_{f,\,nfb}/n_{f,total}$ ratio is for all applied number of cycles. This means that, over the entire fatigue life, most fibers show only one break and the fragmentation of single fibers (i.e., two or more breaks in a single fiber) occurs less frequently. This is in agreement with the observations described in section 3.1.

On the other hand, another important parameter to be quantified is the development of clusters of adjacent fiber breaks through the fatigue life. Fig. 10 shows the evolution of the number of fiber breaks occurring as isolated breaks (i.e., singlets), two adjacent fiber breaks (i.e., doublets), three adjacent fiber breaks (i.e., 3-plets), and so on, for all applied number of cycles, N. As shown in Fig. 10, the higher the number of adjacent fiber breaks, the lower the number of corresponding clusters. This holds valid for all the load levels and number of cycles. Thus, the majority of breaks occur as singlets along the fatigue life, whereas clusters with more than three adjacent fiber breaks occurred very rarely and were mainly concentrated in the regions close to the scrim fibers (see e.g. in Fig. 7-a and 7-c). Unfortunately, it was not possible to identify the maximum number of adjacent fiber breaks because the observations were made on the surface of the specimens and, therefore, possible additional breaks within the material were not detected.

From Figs. 9 and 10 it can be deduced that, under low stress levels (200 and 300 MPa), the damage was not seen to progress either in terms of fragmentation (see Fig. 9) or cluster formation (see Fig. 10). This is due to the absence of propagation of the fiber cracks at the interface or within the matrix. This is made evident by the fact that the plotted curves are not a function of the number of cycles. This suggests that, under such load levels, the material behavior is in line with that postulated by Talreja [4] and by Gamstedt and Talreja [7], according to which, in the so-called "region III" of the fatigue-life diagrams for UD composites under a longitudinal load, the damage introduced at the first cycle is arrested and does not evolve, thus defining a sort of threshold that could be called "fatigue limit". Of course these are only preliminary indications and the problem should be analyzed more extensively and in detail to have a proper statistical relevance of the observations.

Conversely, it can be observed that, for the higher load levels, the damage evolves with the number of cycles, mainly in terms of cluster formation. Such evolution triggers the fatigue failure, even if the final critical mechanism is not yet clear.

Concerning the laminate stiffness, Fig. 11 shows the stiffness curve normalized to the stiffness at the first cycle, $E_1/E_{1,1st\ cycle}$, as a function of the number of cycles for all cases analyzed in this study.

As shown in Fig. 11, regardless of the load level, the stiffness does not seem to decrease substantially. This is reasonably due to the fact that most of the broken fibers have only one break (see Fig. 9). Thus, few fibers are fragmented and the fragmentation length is long. As a consequence, apart from a small region close to the fiber break, the fibers recover their nominal load-bearing capacity and their damage only marginally affects the laminate stiffness. This indicates that, in terms of modelling, it may not be necessary to precisely estimate the fiber breaks to predict the stiffness of composite laminates, at least for low densities of fiber breaks.

4. Conclusions

Experiment-based qualitative and quantitative analyses of the damage initiation and progression in UD glass/epoxy specimens under tension–tension fatigue loading conditions are presented.

In the qualitative analysis, it was shown that the fatigue damage initiates during the first cycle when some fibers fail as a result of the statistical distribution of the fiber strength. Then, from these fiber breaks, either yielding of matrix or fiber/matrix debonding develop depending, among others, on the applied load level. For lower load levels, shear bands in the matrix take place at the fiber crack tip, and fiber/matrix debonds stop growing at a short distance from it. This causes no, or few, new fiber breaks to occur in the neighboring fibers as the number of cycles increases. For higher load levels, in addition to the matrix yielding, fiber/matrix debonds sometimes grow from the fiber crack tip, often reaching neighboring fibers. This results in a redistribution of stresses causing further fiber breaks and, therefore, new matrix yielding or new fiber/matrix debonding throughout the fatigue lifetime. Additionally, it was shown that the damage does not propagate uniformly along the materials. In fact, in regions near the scrim fiber bundles, the damage was seen to develop at a higher rate.

From the quantitative point of view, it was possible to obtain the trend of the probability of survival of the fibers, it decreasing for stress levels higher than 200 MPa, even if most of the damage seemed to be due to the first load application (i.e., first cycle). It was also shown that fiber fragmentation occurs even if most fibers have only one break. As a consequence, the stiffness did not change throughout the fatigue lifetime, as most of the fibers maintain or recover their nominal load-bearing capacity, apart from a small ineffective length. The presence of broken fiber clusters was also analyzed, showing that evolution of such clusters occurred for the highest load levels (320 and 340 MPa), even although most of the breaks occurred as singlets. In contrast, the clustering propagation was totally absent for the lower load levels (200 and 300 MPa), indicating the possible presence of a fatigue threshold.

As these conclusions are based on observations obtained on a laminate surface, further experimental studies may be needed involving the 3D analysis of the bulk material under the same loading conditions

to confirm the findings.

Acknowledgments

This work was part of a Ph.D. external stay by Oscar Castro at the University of Padova, which provided all materials and facilities to develop this research. The Ph.D. project is supported by the Danish Centre for Composite Structures and Materials for Wind Turbines (DCCSM), grant no. 09-067212 from the Danish Strategic Research Council. Financial support from Otto Mønsteds Fond is also gratefully acknowledged.

References

[1] M. Quaresimin, Multiaxial fatigue of composites: experimental evidences and life prediction methodology, in: C.H. Zweben, P. Beaumont (Eds.), Comprehensive Composite Materials II, vol. 2, Elsevier Ltd, 2018, pp. 249–273.
[2] P.A. Carraro, L. Maragoni, M. Quaresimin, Prediction of the crack density evolution in multidirectional laminates under fatigue loadings, Compos. Sci. Technol. 145 (2017) 24–39.
[3] M. Quaresimin, A damage-based approach for the fatigue design of composite structures, IOP Conf. Ser. Mater. Sci. Eng. 139 (2016) 1–12.
[4] R. Talreja, Fatigue of composite materials: damage mechanisms and fatigue-life diagrams, Proc. Roy. Soc. Lond. A. 378 (1981) 461–475.
[5] W.W. Feng, et al., Damage development near the edges of a composite specimen during quasi-static and fatigue loading, J. Compos. Technol. Res. 6 (1984) 3–9.
[6] L. Lorenzo, H.T. Hahn, Fatigue Failure Mechanisms in Unidirectional Composites, ASTM Special Technical Publication, 1986, pp. 210–232.
[7] E.K. Gamstedt, R. Talreja, Fatigue damage mechanisms in unidirectional carbon-fibre-reinforced plastics, J. Mater. Sci. 34 (1999) 2535–2546.
[8] E.K. Gamstedt, L.A. Berglund, T. Peijs, Fatigue mechanisms in unidirectional glass-fibre-reinforced polypropylene, Compos. Sci. Technol. 59 (1999) 759–768.
[9] K. Gamstedt, Effects of debonding and fiber strength distribution on fatigue-damage propagation in carbon fiber-reinforced epoxy, J. Appl. Polym. Sci. 76 (2000) 457–474.
[10] L. Zhuang, R. Talreja, J. Varna, Tensile failure of unidirectional composites from a local fracture plane, Compos. Sci. Technol. 133 (2016) 119–127.
[11] D.R.-B. Aroush, E. Maire, C. Gauthier, S. Youssef, P. Cloetens, H.D. Wagner, A study of fracture of unidirectional composites using in situ high-resolution synchrotron X-ray microtomography, Compos. Sci. Technol. 66 (2016) 1348–1353.
[12] T. Ohsawa, A. Nakayama, M. Miwa, A. Hasegawa, Temperature-dependence of critical fiber length for glass fiber-reinforced thermosetting resins, J. Appl. Polym. Sci. 22 (1978) 3203–3212.
[13] A.N. Netravali, R.B. Henstenburg, S.L. Phoenix, P. Schwartz, Interfacial shear strength studies using the single-filament-composite test. I: experiments on graphite fibers in epoxy, Composites 21 (1990) 226–241.
[14] R.J. Young, C. Thongpin, J.L. Stanford, P.A. Lovell, Fragmentation analysis of glass fibres in model composites through the use of Raman spectroscopy, Compos. Part A Appl. Sci. Manuf. 32 (2001) 253–269.
[15] B.W. Kim, J.A. Nairn, Observations of fiber fracture and interfacial debonding phenomena using the fragmentation test in single fiber composites, J. Compos. Mater. 36 (2002) 1825–1858.
[16] R.B. Henstenburg, S.L. Phoenix, Interfacial shear strength studies using the single-filament-composite test. II. A probability model and Monte Carlo simulation, Polym. Compos. 10 (1989) 389–408.
[17] W.A. Curtin, Exact theory of fibre fragmentation in a single-filament composite, J. Mater. Sci. 26 (1991) 5239–5253.
[18] C.Y. Hui, S.L. Phoenix, M. Ibnabdeljalil, R.L. Smith, An exact closed form solution for fragmentation of Weibull fibers in a single filament composite with applications to fiber-reinforced ceramics, J. Mech. Phys. Solid. 43 (1995) 1551–1585.
[19] R. Gulino, S.L. Phoenix, Weibull strength statistics for graphic fibres measured from the break progression in a model graphite/glass/epoxy microcomposite, J. Mater. Sci. 26 (1991) 3107–3118.
[20] Z.-F. Li, D.T. Grubb, S.L. Phoenix, Fiber interactions in the multi-fiber composite fragmentation test, Compos. Sci. Technol. 54 (1995) 251–266.
[21] Y. Swolfs, et al., Synchrotron radiation computed tomography for experimental validation of a tensile strength model for unidirectional fibre-reinforced composites, Compos. Part A Appl. Sci. Manuf. 77 (2015) 106–113.
[22] P.W.J. Van Den Heuvel, Y.J.W. Van Der Bruggen, T. Peijs, Failure phenomena in multi-fibre model composites: Part 1. An experimental investigation into the influence of fibre spacing and fibre-matrix adhesion, Compos. Part A Appl. Sci. Manuf. 27 (1996) 855–859.
[23] I.J. Beyerlein, S.L. Phoenix, Statistics for the strength and size effects of micro-composites with four carbon fibers in epoxy resin, Compos. Sci. Technol. 56 (1996) 75–92.
[24] M.G. Bader, Tensile strength of uniaxial composites, Sci. Eng. Compos. Mater. 1 (1988) 7–9.
[25] R.L. Smith, A probability model for fibrous composites with local load sharing, Proc. Roy. Soc. Lond. Ser. A Math. Phys. Eng. Sci. 372 (1980) 539–553.
[26] J.M. Neumeister, A constitutive law for continuous fiber-reinforced brittle-matrix composites with fiber fragmentation and stress recovery, J. Mech. Phys. Solid. 41 (1993) 1383–1404.
[27] A. Pupurs, J. Varna, Energy release rate based fiber/matrix debond growth in fatigue. Part I: self-similar crack growth, Mech. Adv. Mater. Struct. 20 (2013) 276–287.
[28] S.C. Garcea, M.N. Mavrogordato, A.E. Scott, I. Sinclair, S.M. Spearing, Fatigue micromechanism characterisation in carbon fibre reinforced polymers using synchrotron radiation computed tomography, Compos. Sci. Technol. 99 (2014) 23–30.
[29] S.C. Garcea, I. Sinclair, S.M. Spearing, In situ synchrotron tomographic evaluation of the effect of toughening strategies on fatigue micromechanisms in carbon fibre reinforced polymers, Compos. Sci. Technol. 109 (2015) 32–39.
[30] S.C. Garcea, I. Sinclair, S.M. Spearing, Fibre failure assessment in carbon fibre reinforced polymers under fatigue loading by synchrotron X-ray computed tomography, Compos. Sci. Technol. 133 (2016) 157–164.
[31] S.C. Garcea, I. Sinclair, S.M. Spearing, P.J. Withers, Mapping fibre failure in situ in carbon fibre reinforced polymers by fast synchrotron X-ray computed tomography, Compos. Sci. Technol. 149 (2017) 81–89.
[32] J. Zangenberg, P. Brøndsted, J.W. Gillespie Jr., Fatigue damage propagation in unidirectional glass fibre reinforced composites made of a non-crimp fabric, J. Compos. Mater. 48 (2014) 2711–2727.
[33] K.M. Jespersen, J. Zangenberg, T. Lowe, P.J. Withers, L.P. Mikkelsen, Fatigue damage assessment of uni-directional non-crimp fabric reinforced polyester composite using X-ray computed tomography, Compos. Sci. Technol. 136 (2016) 94–103.
[34] K.L. Reifsnider, K. Schulte, J.C. Duke, Long-term Fatigue Behavior of Composite Materials, Astm Special Technical Publication, 1983, pp. 136–159.
[35] M. Alves, S. Pimenta, A computationally-efficient micromechanical model for the fatigue life of unidirectional composites under tension-tension loading, Int. J. Fatig. 116 (2018) 677–690.
[36] M. Quaresimin, P.A. Carraro, L. Maragoni, Early stage damage in off-axis plies under fatigue loading, Compos. Sci. Technol. 128 (2016) 147–154.
[37] L. Maragoni, P.A. Carraro, M. Quaresimin, Effect of voids on the crack formation in a [45/-45/0](s) laminate under cyclic axial tension, Compos. Part A Appl. Sci. Manuf. 91 (2016) 493–500.
[38] L. Maragoni, P.A. Carraro, M. Quaresimin, Development, validation and analysis of an efficient micro-scale representative volume element for unidirectional composites, Compos. Part A Appl. Sci. Manuf. 110 (2018) 268–283.
[39] L. Zhuang, A. Pupurs, J. Varna, Z. Ayadi, Effect of fiber clustering on debond growth energy release rate in UD composites with hexagonal packing, Eng. Fract. Mech. 161 (2016) 76–88.
[40] J.A. Nairn, Y.C. Liu, Stress transfer into a fragmented, anisotropic fiber through an imperfect interface, Int. J. Solid Struct. 34 (1997) 1255–1281.
[41] D. Tripathi, F.R. Jones, Single fibre fragmentation test for assessing adhesion in fibre reinforced composites, J. Mater. Sci. 33 (1998) 1–16.
[42] J.F. Mandell, F.J. McGarry, A.J.Y. Hsieh, C.G. Li, Tensile fatigue of glass fibers and composites with conventional and surface compressed fibers, Polym. Compos. 6 (1985) 168–174.